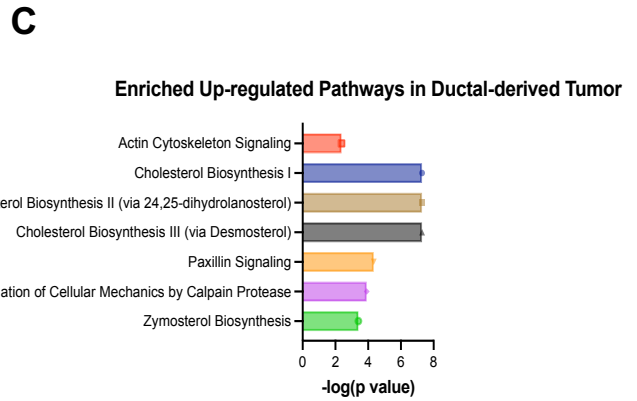## A

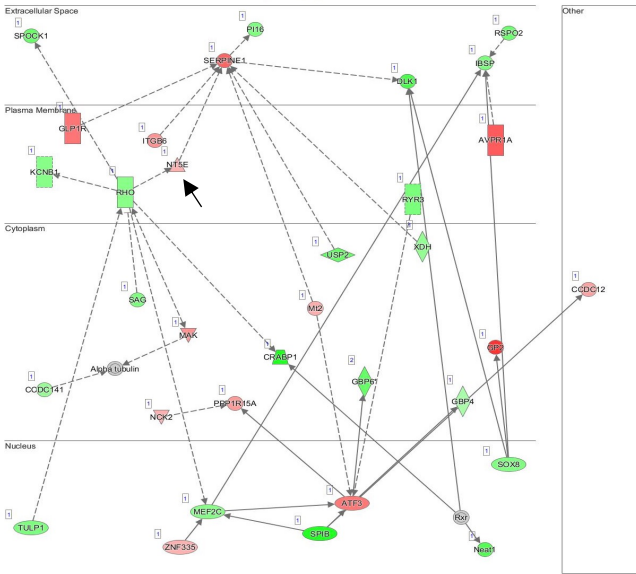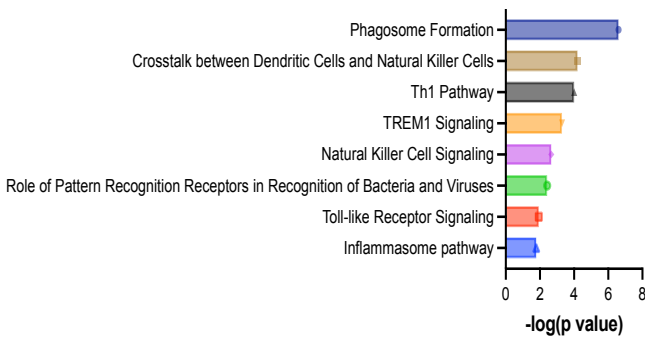**IPA Top Disease and Function Analysis**
Hereditary disorder, Ophthalmic Disease, Organismal Injury and Abnormalities

B

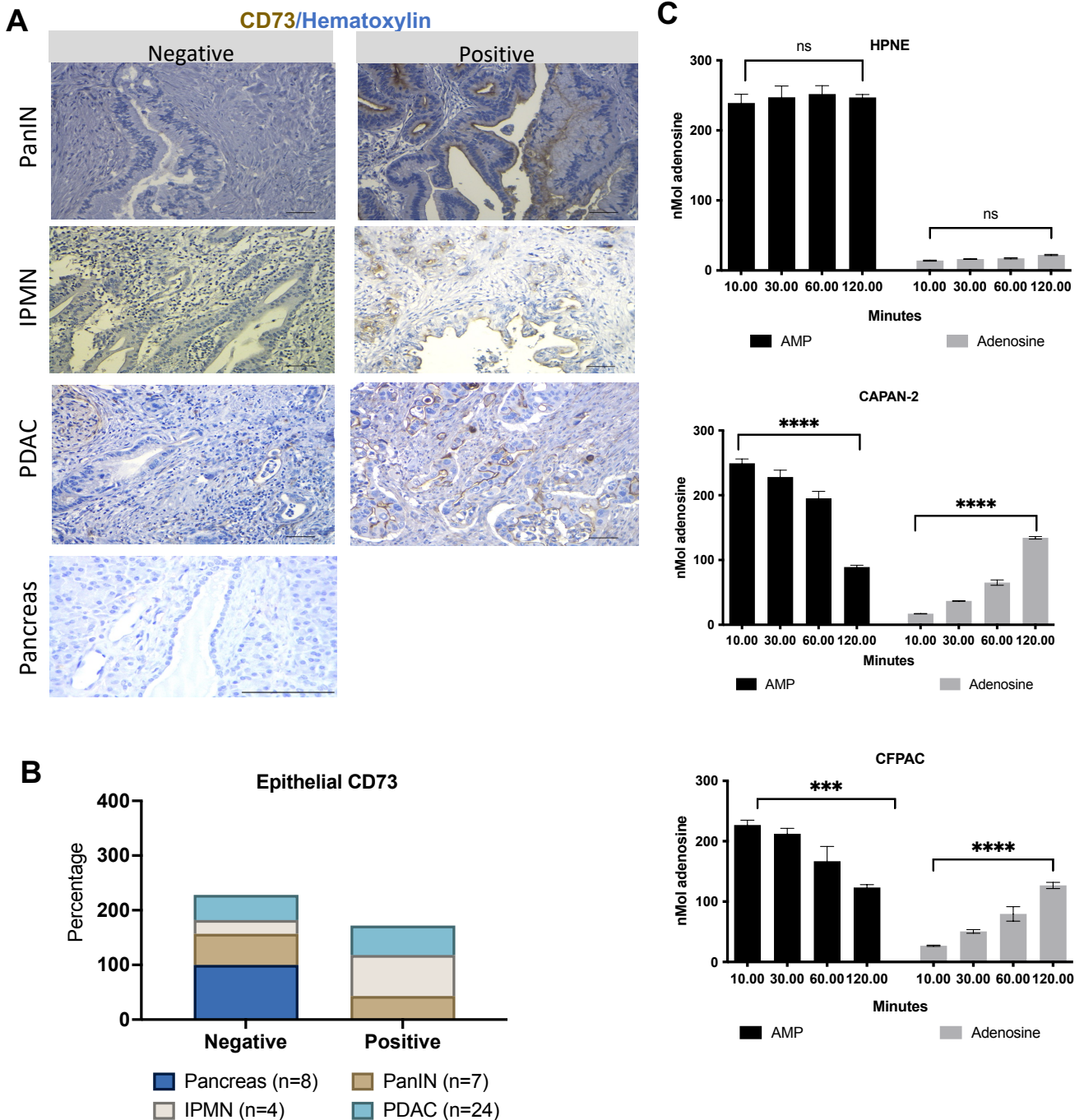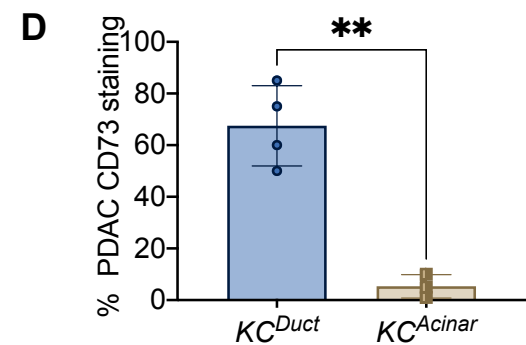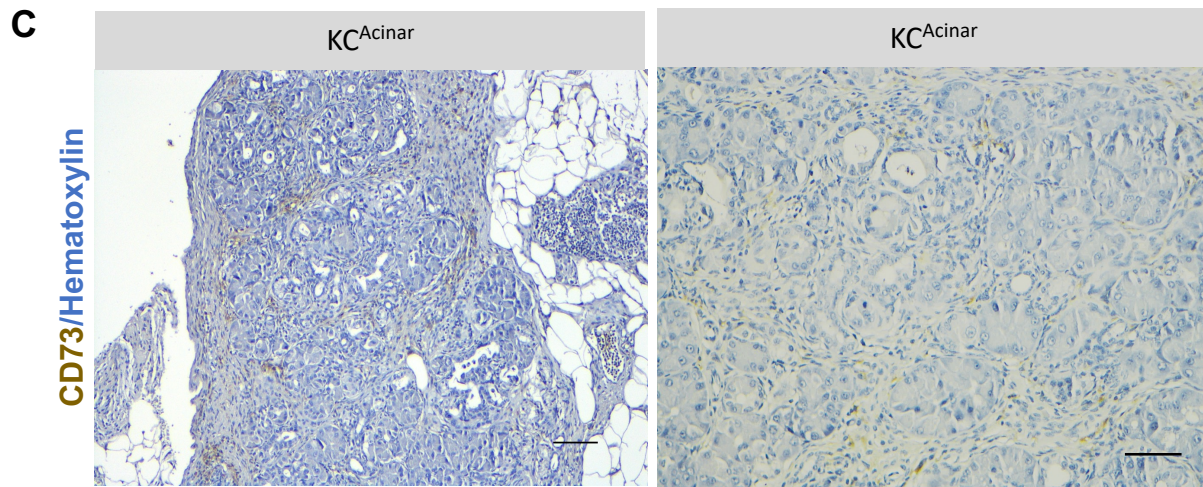**Enriched Down-regulated Pathways in Ductal-derived Tumor**

C

Enriched Up-regulated Pathways in Ductal-derived Tumor

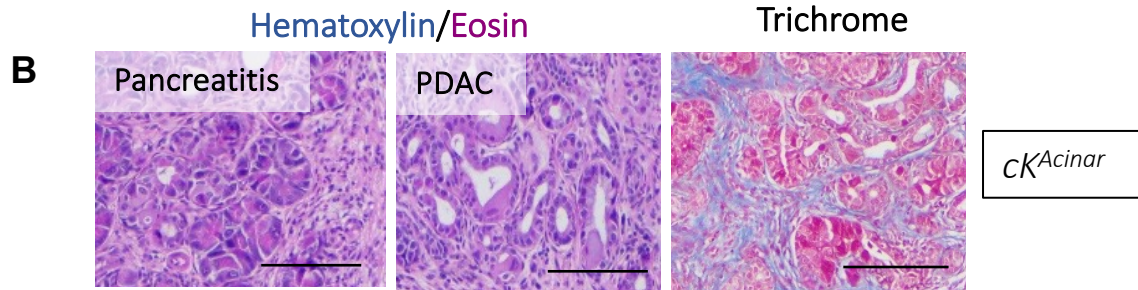**Supplementary Fig. S1 A)** IPA diagram of Hereditary disorder, Ophthalmic Disease, Organismal Injury and Abnormalities, a Top Disease and Function pathway elevated in murine ductal derived tumors. NT5E (arrow) is significantly elevated in this pathway analysis. **B)** IPA comparative analysis of murine KPC[Duct] and KPC[Acinar] RNA-seq signatures. Analysis of whole transcriptomic profiles revealed significant increases in pathways related to cholesterol biosynthesis and **C)** significant decreases in pathways related to innate immunity including Crosstalk between dendritic cells and Th1 Pathway in KPC[Duct] tumors compared to KPC[Acinar] tumors.

Supplemental Fig. S2. A) Immunohistochemical labeling for CD73 in a human PDAC tissue array and resected IPMN. **B)** Quantification of CD73 expressing epithelium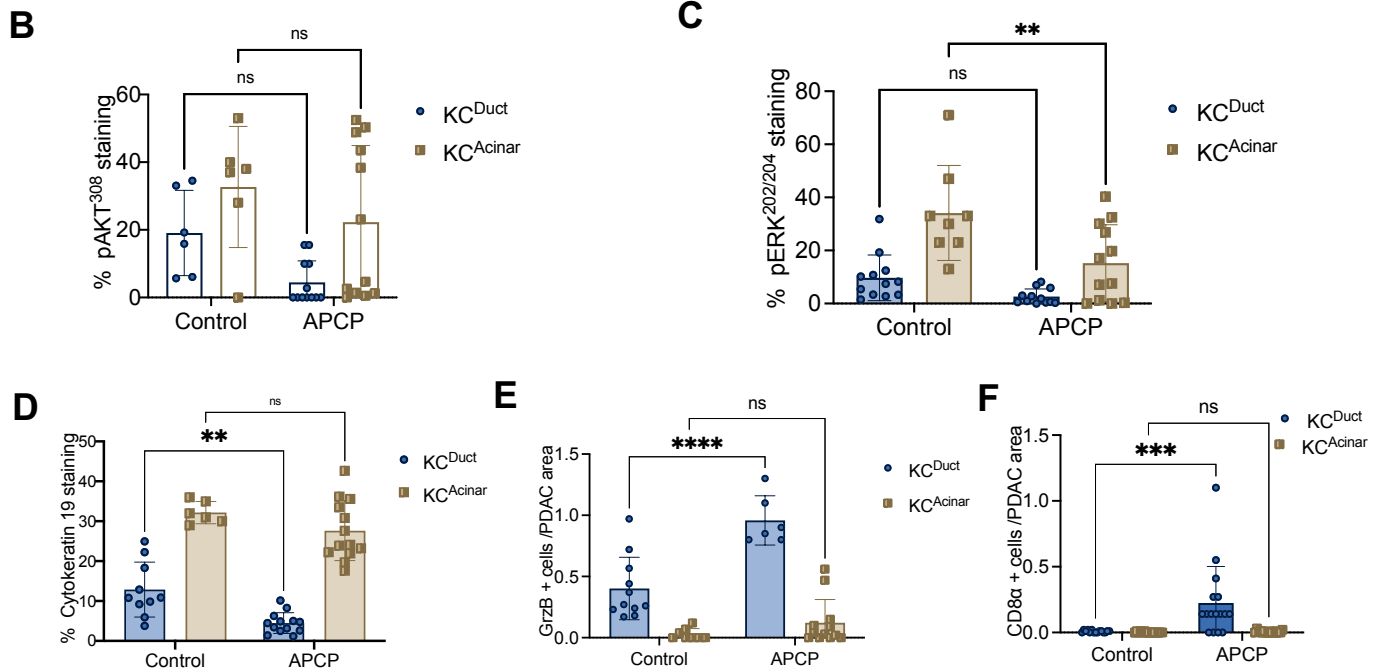. We did not observe CD73 staining in the normal pancreas; however, CD73 is expressed in 54% of PDAC histologic subtypes and 75% of malignant IPMN (scale bars are 50 μm). **C)** To determine if PDAC cell lines had increased CD73 activity, 200 μl of cell line supernatant was analyzed by HPLC or supernatant was replaced with HBSS and 250ng AMP were added. To evaluate CD73 activity, we extracted 100ul of HBSS supernatant at time 0,10, 30, 60 and 120 minutes. CAPAN-2 and CFPAC had significantly increased AMP to Adenosine conversion compared to HPNE cells (****P<0.0001; ***P<0.001). A student's t-test was used to analyze statistics.

A Inducible PanIN/PDAC from acini

Ptf1a:Cre^{ERT2} (Acinar) x ▽ STOP ▽ Kras^{G12V} (Kras) → KC^{Acinar}

TAMOXIFEN (IP)

PROGRESSION   WEEKS

B Hematoxylin/Eosin   Trichrome

Pancreatitis   PDAC

cK^{Acinar}

C CD73/Hematoxylin   KC^{Acinar} KC^{Acinar}

D % PDAC CD73 staining

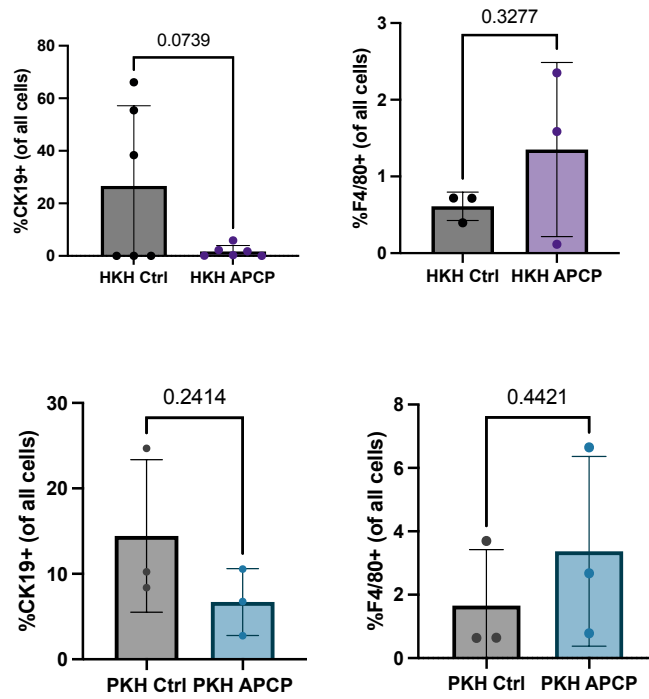KC^{Duct} KC^{Acinar}

**

Supplementary Fig. S3, Histologic analysis of PanIN and stroma in Kras mutant expressing ducts and acini. Oncogenic *Kras* expression significantly increases transcriptomic levels of CD73 A) H&E and Trichrome staining show early and advanced PanIN and collagen deposition adjacent to intraductal PanIN. **B)** H&E and Trichrome staining show early and advanced PanIN and collagen deposition adjacent to PanIN arising in acinar cells. **C)** CD73 IHC staining in KC^{Acinar} sections and **D)** %PDAC CD73 staining in KC^{Duct} compared KC^{Acinar} sections. Increased CD73 staining was found in KC^{Duct} (n= 5) compared to KC^{Acinar} (n= 3) pancreata. Student's t test was used to analyze significance. Scale bars are 50 μm .
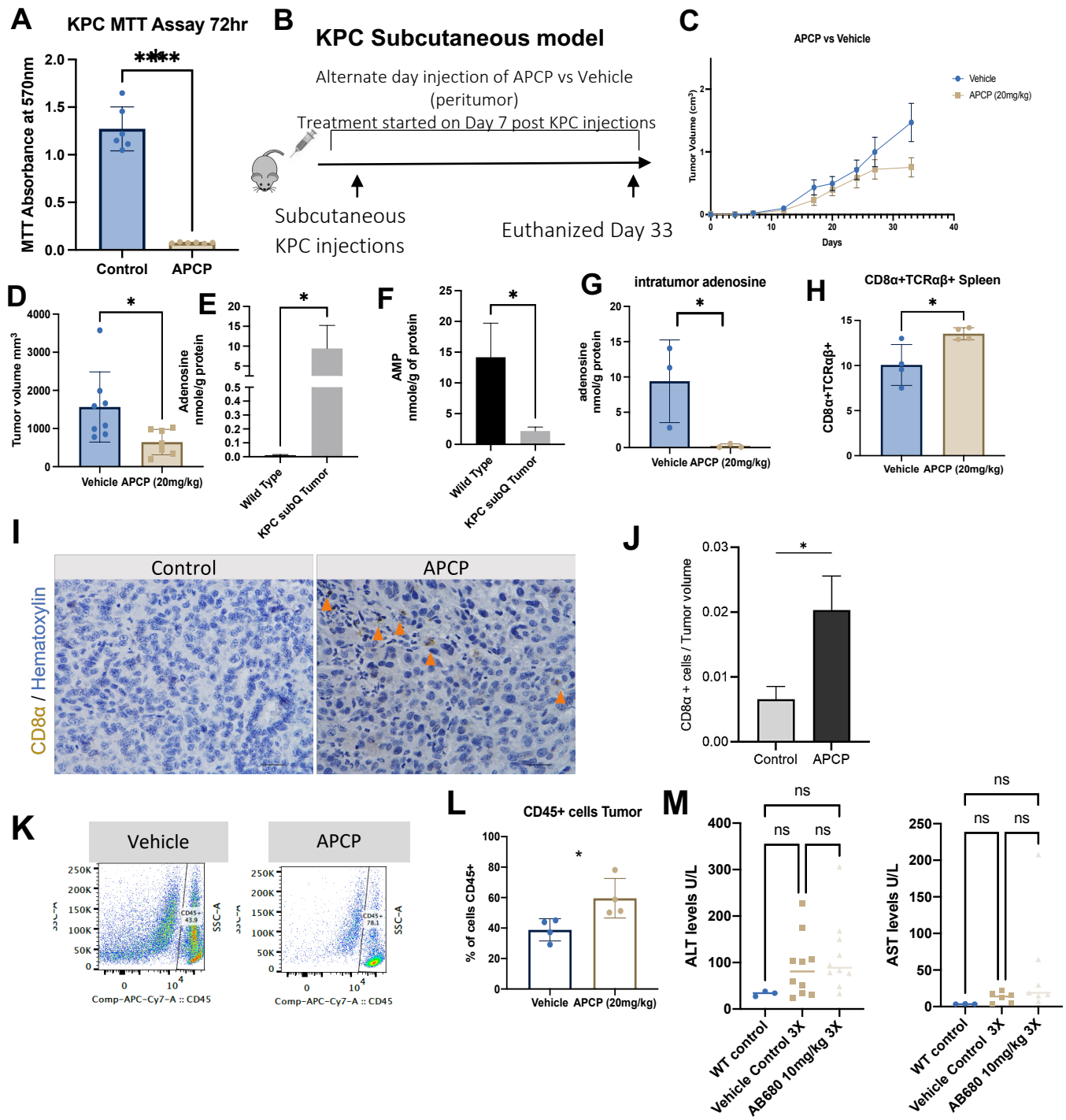
Supplemental Fig. S4. A) Representative CD39 IHC showing in KC[Duct] and KC[Acinar]. **B)** CD39 is not significantly different in the epithelium of KC[Duct] (n= 3) and KC[Acinar] (n= 3). Scale bars are 50 μm.
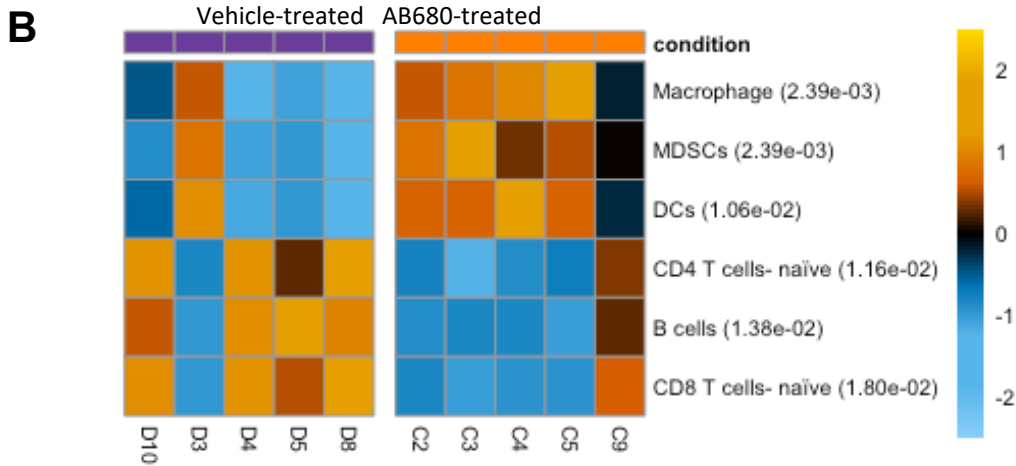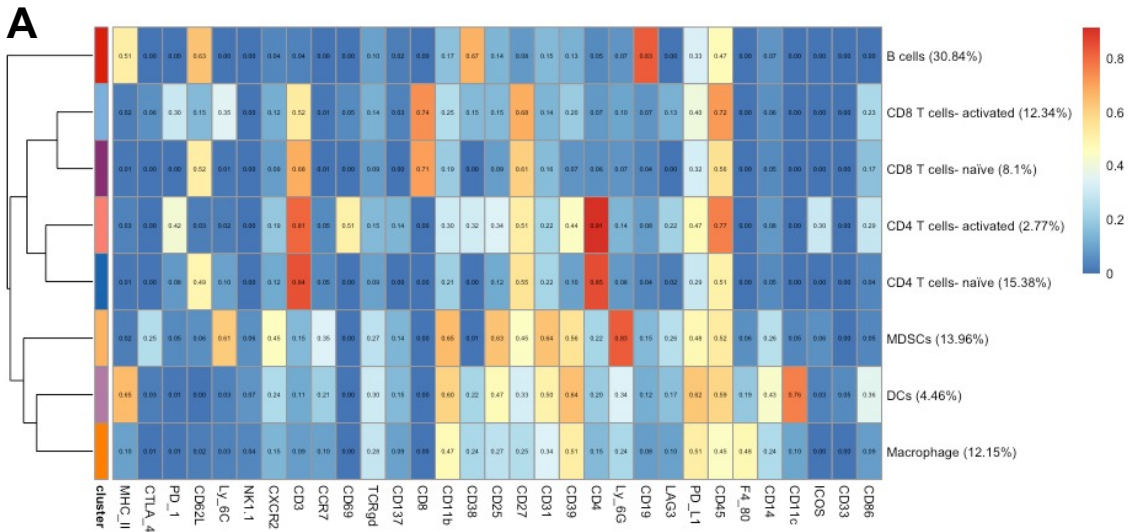
Supplementary Fig. S5 A) Representative IHC for quantification of CK19, p-ERK and p-AKT in Vehicle vs APCP-treated KC^Duct and KC^Acinar GEM models. **B-C)** Inhibition of CD73 reduced the IHC staining intensity of p-ERK$^{202/204}$ and p-AKT^{T308} in KC^Duct pancreata (n= 12) and KC^Acinar pancreata (n=12). **D)** Fold change in %CK19 staining was significantly decreased in APCP-treated KC^Duct mice compared to vehicle control-treated mice. **E)** GZM and **F)** CD8α were significantly increased only in KC^Duct mice (****P<0.0001; ***P<0.001) (n=16 fields analyzed per group and normalized to PDAC area). Scale bars are 50μm. Student's t test or 2-way ANOVA were used to analyze significance.
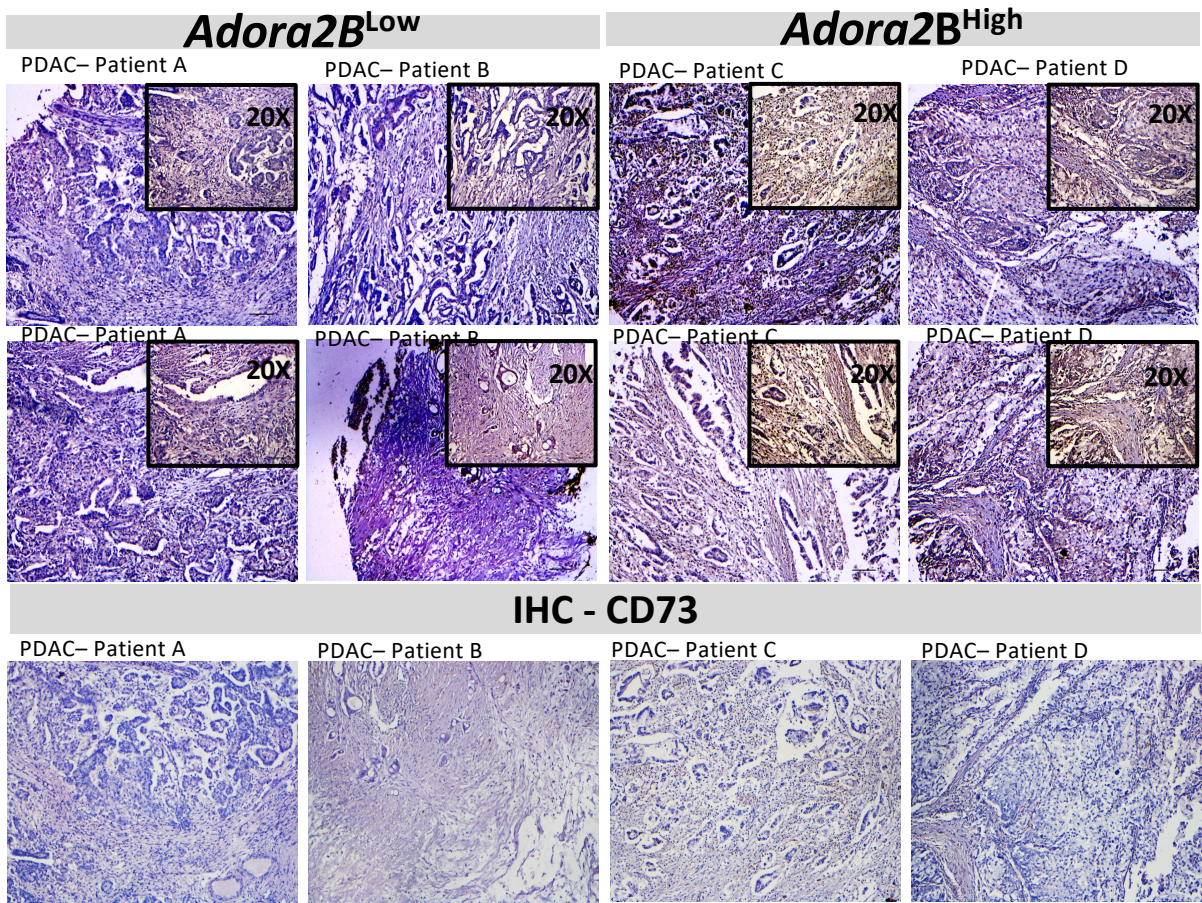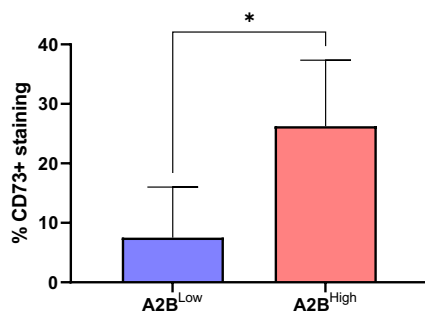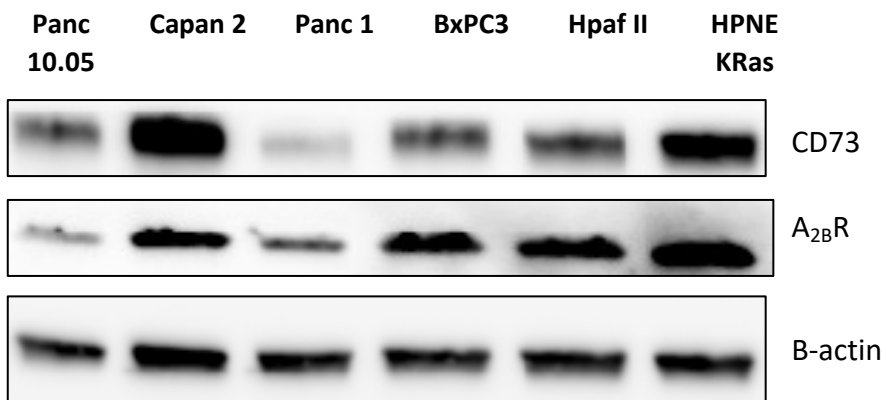
Supplementary Fig. S6 Quantitative multiplex immunoprofiling of CK19+ cells or F4/80+ macrophages of all cells in KC^Duct (HKH) and KC^Acinar (PKH) Control or APCP treated mice. (n=3 per group). A student's t-test using Prism GraphPad software was used for statistical analysis.

Supplementary Fig. S7. Inhibition of CD73 using peritumor delivery of APCP significantly reduced intratumoral adenosine concentrations and elevated anti-tumor immunity. A) MTT assay showing CD73 inhibition significantly reduces KPC proliferation rate *in vitro* (*P<0.001*). **B)** Schematic of KPC subcutaneous tumor injection model. C) APCP treatment significantly decreases KPC subQ tumor growth rates (**P<0.05*) and **D)** final tumor volume (P<0.05). **E)** HPLC analysis of adenosine and AMP levels in KPC subcutaneous tumors compared to wild type pancreata. KPC tumors have significantly increased levels of adenosine and **F)** decreased levels of AMP compared to wild type pancreas *(*P<0.05).* **G)** Inhibition of CD73 significantly reduces intratumoral levels of adenosine *(*P<0.05)* and significantly increases the number of **H)** splenic CD8a+TCRaB+ cells (**P<0.05*). (**I -J**) CD8+ T cells are significantly increased in APCP-treated compared to vehicle-treated tumors (**P<0.05*). **K)** We used FACS to analyze the percentage of CD45+ cells and observed a significant increase in CD45+ cells in tumors from APCP treated mice compared to vehicle treated mice (**L**) (P<0.05) and **M)** No significant difference in serum ALT or AST analysis in AB680 treated mice. Statistical analysis were performed using a student's unpaired t-test in Prism GraphPad software. Scale bars are 50μm

Supplementary Fig. S8 A) Heat Map analysis of CyTOF data showing relative expression of cell clusters. **B**) Quantitative global population analysis reveal increased activated CD4 T cells, CD8 T cells, macrophages and MDSCs.

Supplementary Fig. S9. A) IHC analysis of Adora2b and CD73 expression in a PDAC TMA array. B) Quantification of %CD73+ staining in Adora2b High vs Low patients by IHC. Adora2b High patients have significantly higher %CD73 IHC staining (*$P<0.05$*).t test was performed to analyze significance, n=2 per group. **C)** Western blot showing CD73 and A2BR protein levels in a panel of human PDAC cell lines.